Supplementary Information

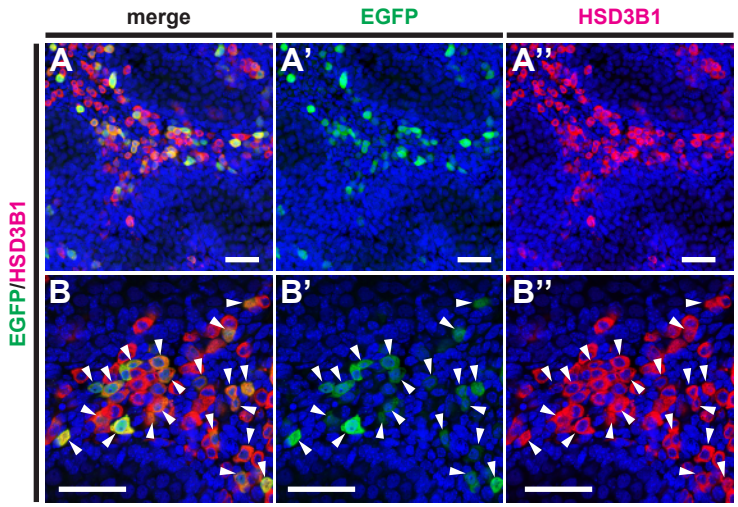

Fig. S1. FLCs labeled by *mFLE-CreERT* in E14.5 testis.

(A, B) Immunostaining of *mFLE-CreERT* (+);*CAG-CAT-EGFP* (+) testis sections with antibodies for EGFP (green) and HSD3B1 (red) at E14.5. The EGFP signals in A and B are shown in A' and B', respectively, while the HSD3B1 signals in A and B are shown in A'' and B'', respectively. White arrowheads in B, B', and B'' indicate colocalization of EGFP and HSD3B1 in FLCs. Bars=50 μm.

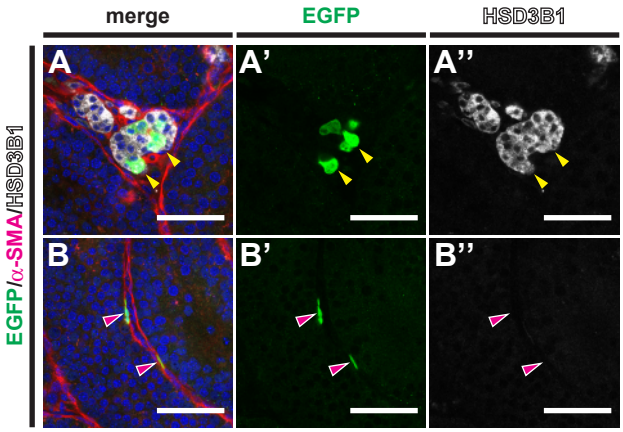

Fig. S2. Characterization of FLCs and their descendant cells in P10 testis.

(A, B) Immunostaining of *mFLE-CreERT* (+);*CAG-CAT-EGFP* (+) testis sections with antibodies for EGFP (green), α-SMA (red), and HSD3B1 (white) at P10. The EGFP signals in A and B are shown in A' and B', respectively, while the HSD3B1 signals in A and B are shown in A'' and B'', respectively. Yellow arrowheads in A, A', and A'' indicate HSD3B1-positive FLCs. Red arrowheads in B, B', and B'' indicate PTMCs that do not express HSD3B1. Bars=50 μm.

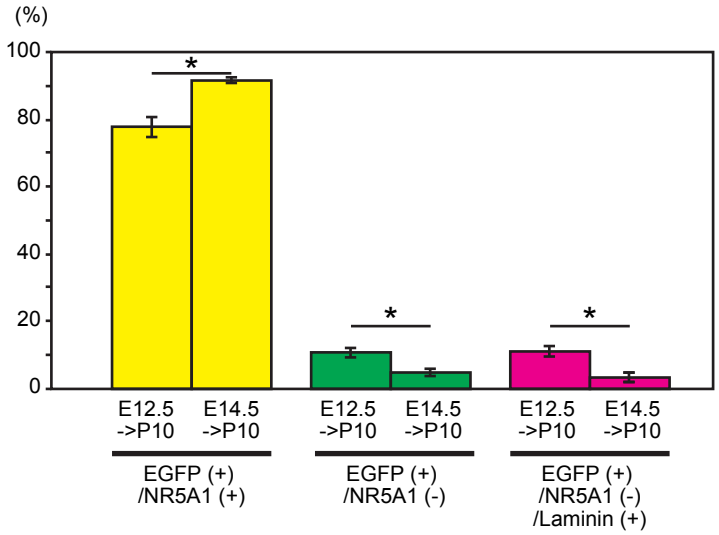

Fig. S3. Comparison of the fate of FLCs labeled at E12.5 or E14.5 in the neonatal testis.

FLCs were labeled at E12.5 or E14.5, and the percentages of the indicated cell populations in the P10 testis were calculated (three sections from three individual mice). We counted 20 to 65 cells in each section and 92 to 149 cells in each sample. The data are presented as means±SEM. *$p < 0.05$.

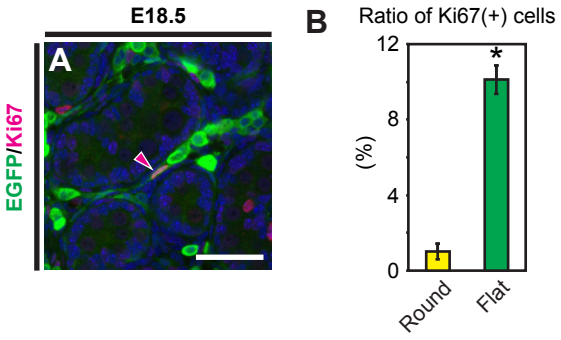

Fig. S4. Dedifferentiated FLCs are proliferating in the fetal testis.

(A) *mFLE-Cre;CAG-CAT-EGFP* mouse testis was immunostained for EGFP (green) and Ki67 (red) at E18.5. The red arrowhead indicates a flat-shaped cell that expresses both EGFP and Ki67. Bar=50 μm **(B)** Percentages of Ki67-positive cells in the round-shaped EGFP-positive cells and flat-shaped EGFP-positive cells. We counted 24 to 101 cells in each section (three sections from each sample, n=3). The data are presented as means±SEM. *$p < 0.05$.

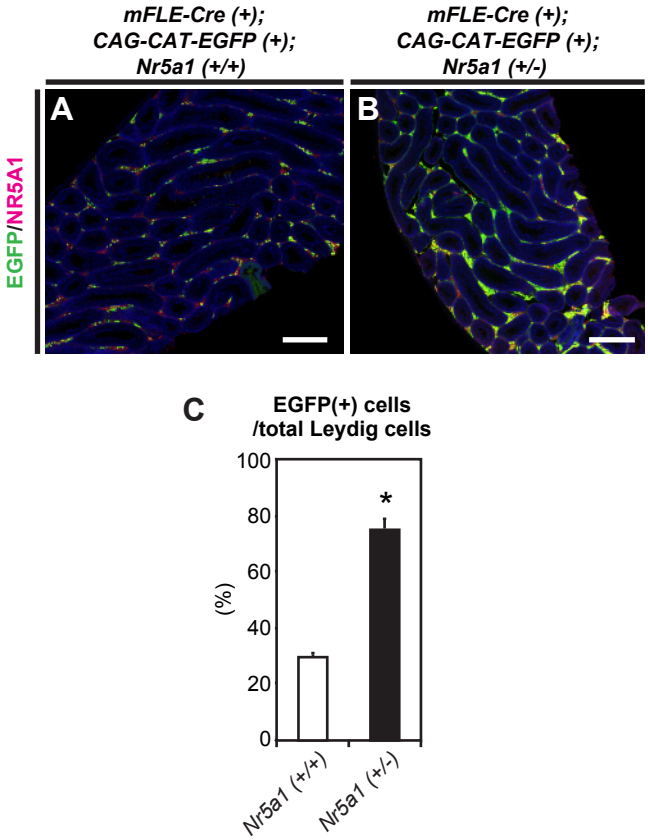

Fig. S5. FLCs and their descendant cells labeled by *mFLE-Cre* in the adult testis.

(A and B) The *mFLE-Cre;CAG-CAT-EGFP;Nr5a1 (+/+)* testis and the *mFLE-Cre;CAG-CAT-EGFP;Nr5a1 (+/-)* testis were subjected to immunostaining for EGFP (green) and NR5A1 (red) at P56. Bars=200μm. **(C)** Percentages of EGFP-positive cells in the NR5A1-positive total Leydig cells. We counted 110 to 223 cells in each section (three sections from each sample, n=3). The data are presented as means±SEM. *$p < 0.05$.

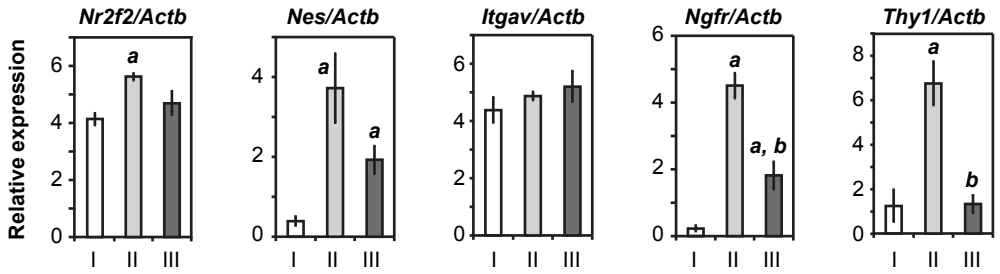

Fig. S6. mRNA expression in cell populations sorted from P10 testis.

Expressions of ALC stem cell marker genes in the sorted cell populations I, II, and III were analyzed by quantitative RT-PCR. Expression level of each gene was standardized by *Actb* (β-actin) expression and presented as means±SEM. Results of the t-test analyses are shown by small italic characters; "*a*" indicates significant difference from population I, while "*b*" indicates significant difference from population II ($p < 0.05$).

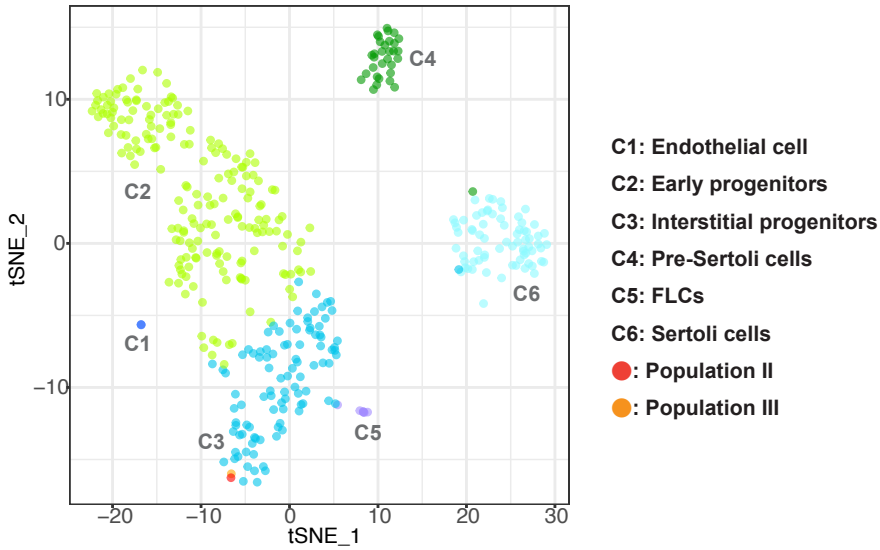

Fig. S7. Comparison of the transcriptomes in the population II and III with the previously reported single cell transcriptomes in the fetal testis.

Transcriptomes in population II and III were compared with those in the fetal testicular cells (Stevant et al., 2018). t-SNE analyses revealed six clusters (C1–C6), and both population II and population III were classified as cluster 3, which contains interstitial progenitor cells in the fetal testis.

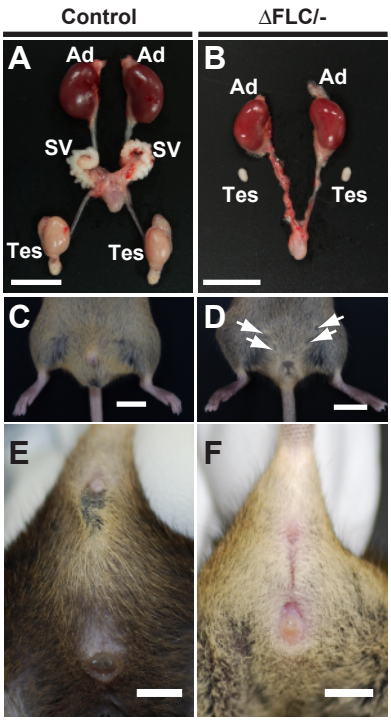

Fig. S8. Phenotypes of ΔFLC/- mouse at P56.

(A and B) Appearance of urogenital tissues isolated from the control male and ΔFLC/- male mice. Ad; adrenal gland, SV; seminal vesicle, Tes; testis. Bars=10 mm. **(C and D)** Appearance of the lower abdomen. Arrows in D indicate nipples. Bars=10 mm. **(E and F)** Appearance of the external genitalia. Bars=5 mm.

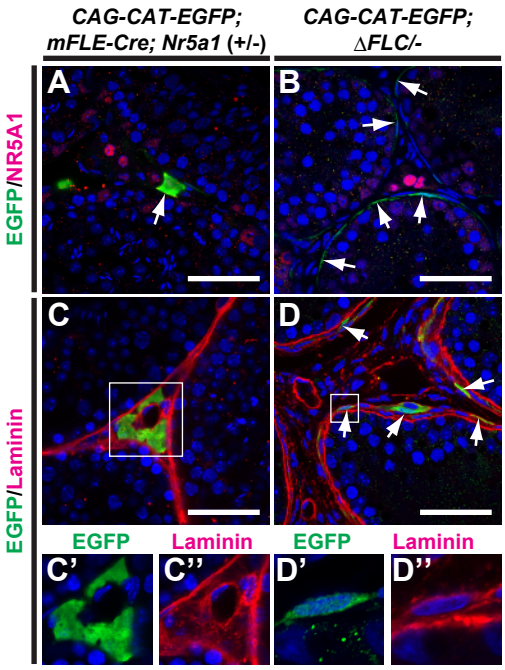

Fig. S9. Persistence of *Nr5a1* gene disrupted cells in the ΔFLC/- mice at P56.

(A and B) Immunostaining of testis sections from control (*CAG-CAT-EGFP;mFLE-Cre;Nr5a1 (+/-)*) mice and *CAG-CAT-EGFP;ΔFLC/-* mice with antibodies for EGFP (green) and NR5A1 (red). Arrows in B indicate EGFP-positive and NR5A1-negative peritubular cells. **(C and D)** Immunostaining of the testis sections with antibodies for EGFP (green) and Laminin (red). Arrows in D indicate EGFP-positive and Laminin-positive peritubular cells. Areas enclosed by open rectangles in C and D were enlarged, and EGFP and Laminin signals are individually shown in C', C'', D', and D''. Bars=50 μm.

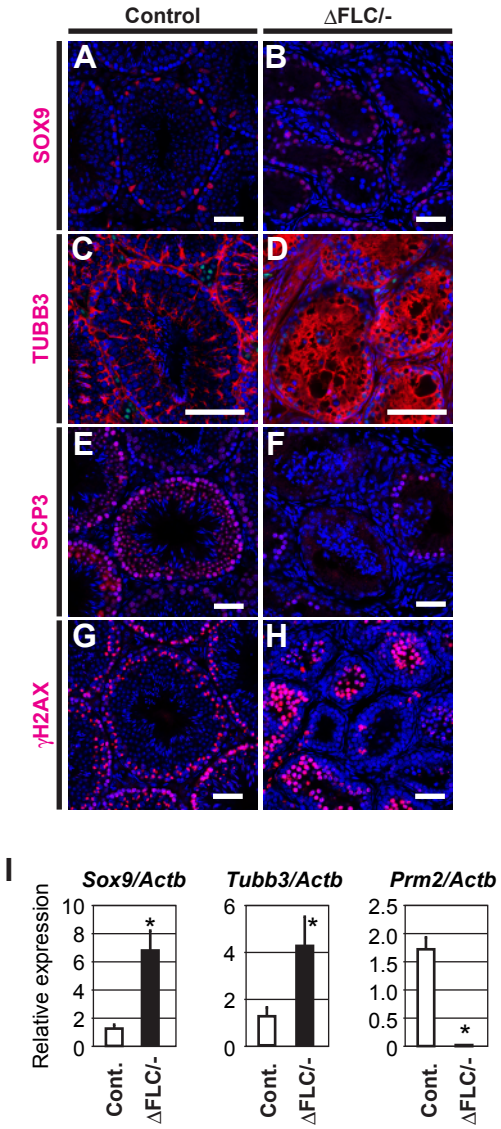

Fig. S10. Sertoli cell polarity and spermatogenesis were affected in the ΔFLC/- mouse at P56.

(A–H) The testis sections from control mice and ΔFLC/- mice were immunostained with antibodies for SOX9 (A and B), TUBB3 (C and D), SCP3 (E and F), and γH2AX (G and H). Bars=50 μm. **(I)** mRNA expressions of *Sox9*, *Tubb3*, and *Prm2* in the control and ΔFLC/- testes were analyzed by quantitative RT-PCR. Expression levels of each gene were standardized by *Actb* (β-actin) expression and presented as means±SEM. **p* < 0.05.

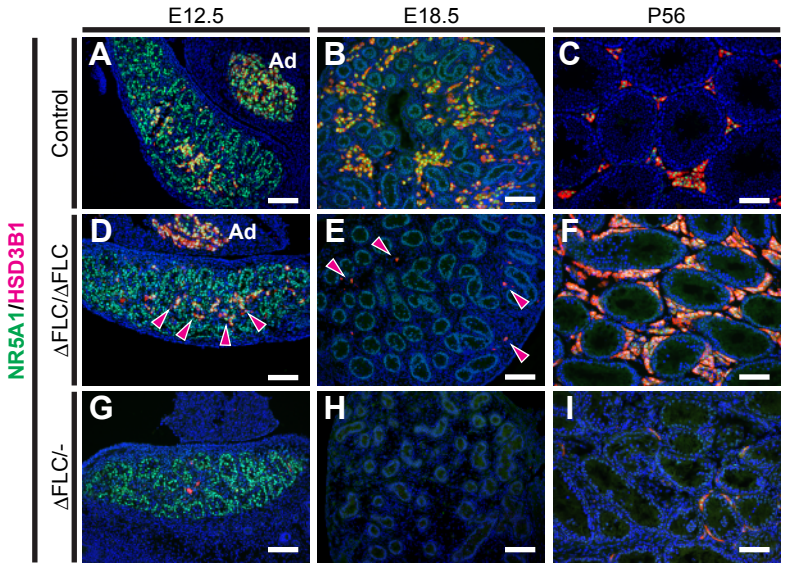

Fig. S11. Leydig cell development in the control, ΔFLC/ΔFLC, and ΔFLC/- mice.

(A–C) Immunostaining of the control mouse testis for NR5A1 (green) and HSD3B1 (red) at E12.5 (A), E18.5 (B), and P56 (C). **(D–F)** Immunostaining of the ΔFLC/ΔFLC mouse testis for NR5A1 (green) and HSD3B1 (red) at E12.5 (D), E18.5 (E), and P56 (F). Red arrowheads in D and E indicate HSD3B1-positive FLCs persisted in the testis. **(G–I)** Immunostaining of the ΔFLC/- mouse testis for NR5A1 (green) and HSD3B1 (red) at E12.5 (G), E18.5 (H), and P56 (J). Ad; adrenal gland. Bars=100 μm.

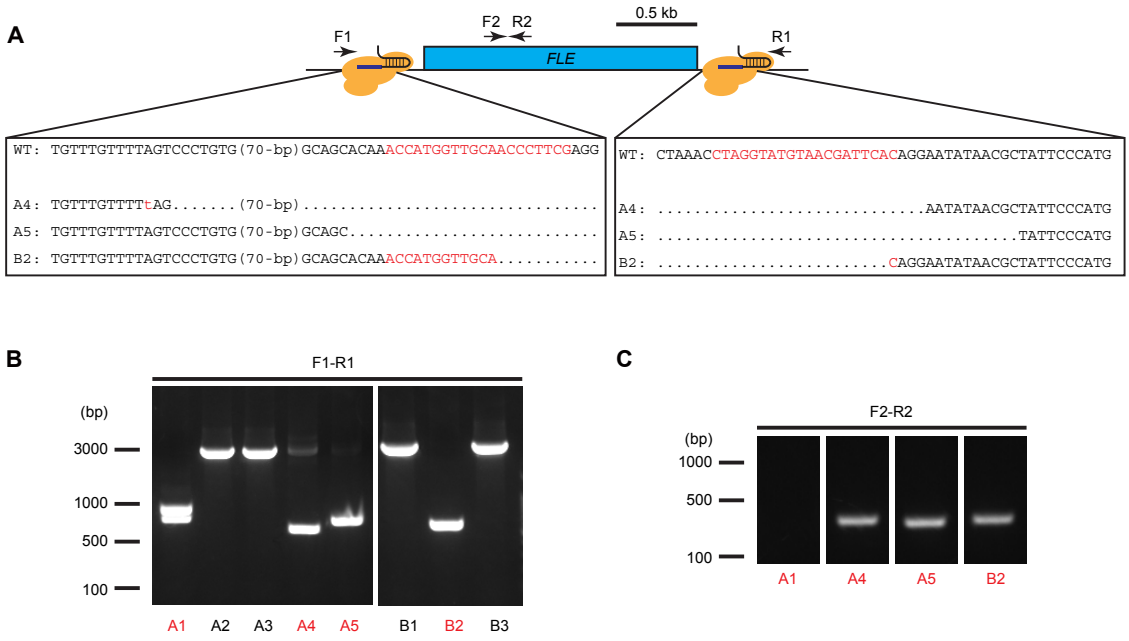

Fig. S12. Generation of ΔFLE mice by CRISPR/Cas9.

(A) Schematic illustration of the strategy to generate ΔFLE mice using CRISPR/Cas9. Two guide RNAs were designed to recognize the sequences located upstream and downstream of FLE. Arrows indicate PCR primers. Nucleotide sequences in the open boxes show deletion patterns in three distinct F0 founders, A4, A5, and B2. Red characters indicate 20-bp target sequences. **(B)** Genotyping PCR of F0 founders with primers F1 and R1. **(C)** Genotyping PCR of F0 founders with primers F2 and R2. The results show that FLE was homozygously deleted in A1, and heterozygously deleted in A4, A5, and B2.

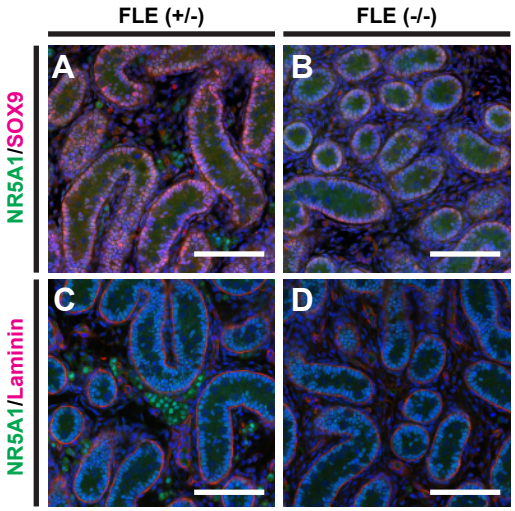

Fig. S13. Sertoli cells and basement membrane in ΔFLE mouse testis at E18.5.

The testis sections from control mice and ΔFLE mice were immunostained with antibodies for NR5A1 (green) and SOX9 (red) (A and B) or NR5A1 (green) and Laminin (red) (C and D) at E18.5. Bars=100 μm.

Table S1: Primary and secondary antibodies used in immunofluorescence analyses.

Primary antibodies

Target protein	Source (reference)	Dilution (sections)	Dilution (free floating)
EGFP	Chicken polyclonal (Abcam; ab13970)	1:1000	1:10000
NR5A1	Rabbit polyclonal (Morohashi et al., 1993)	1:2000	1:20000
NR5A1	Rat monoclonal (Shima et al., 2008; Yokoyama et al., 2009)	-	1:2000
Laminin	Rabbit polyclonal (Sigma-Aldrich; L9393)	1:1000	1:10000
HSD3B1 (3β-HSD type 1)	Rabbit polyclonal (Fatchiyah et al., 2006)	-	1:20000
SOX9	Rabbit polyclonal (Katoh-Fukui et al., 2011)	-	1:20000
PECAM-1	Rat monoclonal (BD Biosciences; MEC13.3)	-	1:10000
ARX	Rabbit polyclonal (Kitamura et al., 2002)	-	1:10000
α-SMA	Rabbit monoclonal (Abcam; ab124964)	-	1:10000
α-SMA	mouse monoclonal (Abcam; ab7817)	-	1:10000
Collagen type IV	Rabbit polyclonal (Abcam; ab6586)	-	1:10000
HSD3B6 (3β-HSD type 6)	Rabbit polyclonal (Yamamura et al., 2014)	1:500	1:5000
TUBB3	Mouse monoclonal (Abcam; ab78078)	-	1:10000
SCP3	Rabbit polyclonal (Abcam; ab15093)	-	1:10000
γH2AX	Rabbit polyclonal (Abcam; ab2893)	-	1:10000
Ki67	Rabbit polyclonal (Abcam; ab15580)	-	1:10000

Secondary antibodies

Target protein	Source	Dilution (section)	Dilution (free floating)
Rabbit IgG	ALEXA Fluor® 488 goat anti-rabbit IgG (H+L) (Life Technologies; A11008)	-	1:500
Rat IgG	ALEXA Fluor® 488 goat anti-rat IgG (H+L) (Life Technologies; A11006)	-	1:500
Rabbit IgG	ALEXA Fluor® 594 goat anti-rabbit IgG (H+L) (Life Technologies; A11012)	1:500	1:500
Rat IgG	ALEXA Fluor® 594 goat anti-rat IgG (H+L) (Life Technologies; A11008)	-	1:500
Mouse IgG	ALEXA Fluor® 555 goat anti-mouse IgG (H+L) (Life Technologies; A21422)	-	1:500
Chicken IgY	Goat anti-chicken IgY H&L (ALEXA Fluor® 488) (Abcam; ab150169)	1:500	1:500
Rabbit IgG	ALEXA Fluor® 647 donkey anti-rabbit IgG (H+L) (Life Technologies; A31573)	1:500	1:500

Table S2: Primers used in quantitative RT-PCR analyses.

Gene (protein)	Primer direction	Primer sequence (5′ - 3′)
Actb (β-actin)	F	AGGGTGTGATGGTGGGAATGG
	R	TGGCTGGGGTGTTGAAGGTCT
Cre	F	GGTTCGTTCACTCATGGAAAAT
	R	GGCAATTTCGGCTATACGTAAC
EGFP	F	TATATCATGGCCGACAAGCA
	R	TGTTCTGCTGGTAGTGGTCG
Nr5a1 (Ad4BP/SF-1)	F	AAGCCACTCTGTAGGACCAAGC
	R	TGTAAATCTGACGCGAAAGCAG
Hsd3b1	F	CAAGTGTGCCAGCCTTCATCT
	R	TTCATGATTCTGTTCCTCGTGG
Insl3 (RLF)	F	ATTGCTCCCCACCTCCTGGCTATG
	R	GGTCATGATGGGGCTTCTTGGGGA
Acta2 (α-SMA)	F	GTTCCTTTGCCTATCAGAATGG
	R	AAAAACACACAAAAACCCAACC
Arx	F	TGCCACTGCCAATGTCACTCCAAC
	R	ATCCGGAGGAAGAGAAGGTTGGGC
Pdgfra	F	CAAACCCTGAGACCACAATGG
	R	TGATGCCCACATAGCCTTCAT
Star	F	TACATCCAGCAGGGAGAGGTG
	R	CAGCGCACGCTCACGAAGTCT
Amh (MIS)	F	GAACCTCTGCCCTACTCGGG
	R	AAGTCCACGGTTAGCACCAAA
Sox9	F	TGTGACACGGGACAACACATG
	R	GGCTATCCACGGCACACAC
Ddx4 (MVH, VASA)	F	GCACACGTTGAATACAGCGGGGAT
	R	TGGGAGGAAGAACAGAAGAACAGG
*Hsd3b6**	F	TTTTTTTGAGGTATTGACAAGTATTTATTG
	R	TCCCCATTCAGAGCATGTATAGC
Hsd17b3	F	ATGGAGTCAAGGAGGAAAGGC
	R	GGCTGTAAAGAGGCCAGGG
Sult1e1 (EST)	F	ATCATTTCACTTCTTCCACGGG
	R	ACTCCACGGAACTCTCCAAAAA
Ptgds (PGD2, PGDS)	F	AAGGGCCCAGGCCAGGACTT
	R	TGCACTTATCCGGTTGGGGCAG
Nr2f2 (COUP-TFII)	F	TGCGGAGGAACCTGAGCTAC
	R	CTGTACAGCTTCCCGTCTCAT
Nes	F	GGGAGAGTCGCTTAGAGGTG
	R	ACAGCCAGCTGGAACTTTTC
Itgav	F	AACCCTGAGACTGAAGAAGACG
	R	TTTGTAAGGCCACTGGAGATTT
Ngfr	F	CATAGGATGGTAAAGCCCAGAG
	R	TTCCAGATGTTTCCCTGAAAGT
Thy1 (CD90)	F	GGAAGATAGCTTTCCCAAGGAT
	R	TCCAGAGGCTTGGTTTTATTGT
Cyp11a1 (P450SCC)	F	CGAATCGTCCTAAACCAAGAG
	R	CACTGATGACCCCTGAGAAAT
Cyp17a1	F	GGGTGACCCCAAGGTGGTCTTTCT
	R	TGGGATCCGGGACGTTAGATTCGG
Tubb3	F	CATCCAGAGTAAGAACAGCAGC
	R	GTGAACTCCATCTCATCCATGC
Prm2	F	GCATCGCAGAGGCTGCAGAAGA
	R	GCAGAATGGACAGGCCTGGGG

*Primers for Hsd3b6 were originally designed by O' Shaughnessy PJ, *et al.* (O'Shaughnessy et al., 2002).

Table S3: Nucleotide sequences of guide RNAs used for genome editing experiments and PCR primers for genotyping the mice generated by genome editing.

Guide RNAs

Guide RNA name	Sequence*
FLE-gRNA-up	ACCATGGTTGCAACCCTTCGagg
FLE-gRNA-down	CTAGGTATGTAACGATTCACagg

*Small characters represent protospacer adjacent motif sequences.

Genotyping PCR primers

Primer name	Sequence	Amplicon
FLE-Fw1	TTAGAGCATGCAGGTATAGCAGAG	WT: 2899 bp
FLE-Re1	CTGTTGAATGCATATCTGAAGGTC	del: 615 bp
FLE-Fw2	AAGGGATGAACACTAAGGGGTT	WT: 234 bp
FLE-Re2	CTTGTGGAGGCAATGTGTAGAG	del: -

Table S4: mRNA expression profiles in the cell population II (P10_EGFP+Laminin-) and the cell population III (P10_EGFP+Laminin+) revealed by mRNA-sequence analyses.

Click here to Download Table S4

References for Supplementary Information

Fatchiyah, Zubair, M., Shima, Y., Oka, S., Ishihara, S., Fukui-Katoh, Y. and Morohashi, K. (2006). Differential gene dosage effects of Ad4BP/SF-1 on target tissue development. *Biochem Biophys Res Commun* **341**, 1036-1045.

Katoh-Fukui, Y., Miyabayashi, K., Komatsu, T., Owaki, A., Baba, T., Shima, Y., Kidokoro, T., Kanai, Y., Schedl, A., Wilhelm, D., et al. (2011). Cbx2, a Polycomb Group Gene, Is Required for Sry Gene Expression in Mice. *Endocrinology*.

Kitamura, K., Yanazawa, M., Sugiyama, N., Miura, H., Iizuka-Kogo, A., Kusaka, M., Omichi, K., Suzuki, R., Kato-Fukui, Y., Kamiirisa, K., et al. (2002). Mutation of ARX causes abnormal development of forebrain and testes in mice and X-linked lissencephaly with abnormal genitalia in humans. *Nat Genet* **32**, 359-369.

Morohashi, K., Zanger, U. M., Honda, S., Hara, M., Waterman, M. R. and Omura, T. (1993). Activation of CYP11A and CYP11B gene promoters by the steroidogenic cell-specific transcription factor, Ad4BP. *Mol Endocrinol* **7**, 1196-1204.

O'Shaughnessy, P. J., Willerton, L. and Baker, P. J. (2002). Changes in Leydig cell gene expression during development in the mouse. *Biol Reprod* **66**, 966-975.

Shima, Y., Zubair, M., Komatsu, T., Oka, S., Yokoyama, C., Tachibana, T., Hjalt, T. A., Drouin, J. and Morohashi, K. (2008). Pituitary homeobox 2 regulates adrenal4 binding protein/steroidogenic factor-1 gene transcription in the pituitary gonadotrope through interaction with the intronic enhancer. *Mol Endocrinol* **22**, 1633-1646.

Stevant, I., Neirijnck, Y., Borel, C., Escoffier, J., Smith, L. B., Antonarakis, S. E., Dermitzakis, E. T. and Nef, S. (2018). Deciphering Cell Lineage Specification during Male Sex Determination with Single-Cell RNA Sequencing. *Cell Rep* **22**, 1589-1599.

Yamamura, K., Doi, M., Hayashi, H., Ota, T., Murai, I., Hotta, Y., Komatsu, R. and Okamura, H. (2014). Immunolocalization of murine type VI 3beta-hydroxysteroid dehydrogenase in the adrenal gland, testis, skin, and placenta. *Molecular and cellular endocrinology* **382**, 131-138.

Yokoyama, C., Komatsu, T., Ogawa, H., Morohashi, K., Azuma, M. and Tachibana, T. (2009). Generation of rat monoclonal antibodies specific for Ad4BP/SF-1. *Hybridoma (Larchmt)* **28**, 113-119.